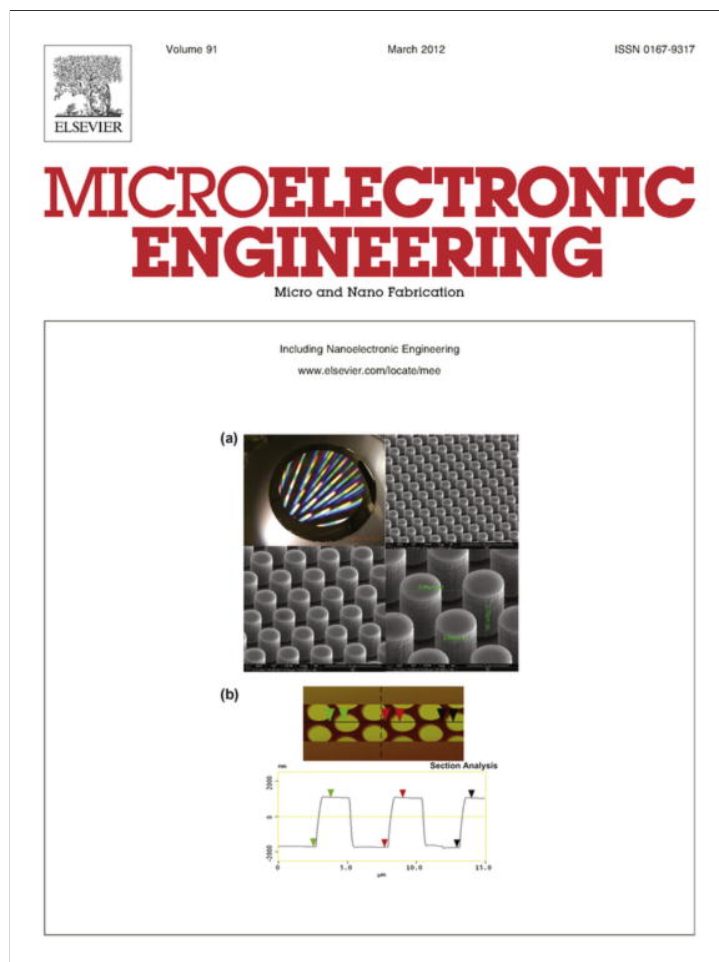


Provided for non-commercial research and education use.  
Not for reproduction, distribution or commercial use.



(This is a sample cover image for this issue. The actual cover is not yet available at this time.)

This article appeared in a journal published by Elsevier. The attached copy is furnished to the author for internal non-commercial research and education use, including for instruction at the authors institution and sharing with colleagues.

Other uses, including reproduction and distribution, or selling or licensing copies, or posting to personal, institutional or third party websites are prohibited.

In most cases authors are permitted to post their version of the article (e.g. in Word or Tex form) to their personal website or institutional repository. Authors requiring further information regarding Elsevier's archiving and manuscript policies are encouraged to visit:

<http://www.elsevier.com/copyright>



Contents lists available at SciVerse ScienceDirect

## Microelectronic Engineering

journal homepage: [www.elsevier.com/locate/mee](http://www.elsevier.com/locate/mee)

## A 2D MEMS grating based CMOS compatible poly-SiGe variable optical attenuator

S. Rudra<sup>a,\*</sup>, R. Van Hoof<sup>b</sup>, J. De Coster<sup>b</sup>, G. Bryce<sup>b</sup>, S. Severi<sup>b</sup>, A. Witvrouw<sup>b</sup>, D. Van Thourhout<sup>a</sup><sup>a</sup> Photonics Research Group, INTEC, Ghent University – IMEC, Gent, Belgium<sup>b</sup> IMEC, Leuven, Belgium

## ARTICLE INFO

## Article history:

Received 28 June 2012

Received in revised form 20 November 2012

Accepted 7 December 2012

Available online 5 January 2013

## Keywords:

Micro-opto-electro-mechanical systems (MOEMS)

Variable optical attenuator (VOA)

Grating

Monolithic integration

## ABSTRACT

A variable optical attenuator based on a 2D MEMS grating is described. The device is a perforated and suspended poly-SiGe membrane with fixed islands within the perforations. It specularly reflects light in the non-actuated state, whereas after actuation the membrane deflects downwards forming a grating which diffracts light in higher orders reducing the intensity of the specular reflection. Using a laser of 400 nm wavelength, we could obtain an attenuation level of 20 dB with 0.11 dB of polarization dependent loss. A close match was obtained between the experimental and simulated mechanical behavior of the device showing the possibility of efficiently extending its use in the NIR regime. Additionally, as the device is made of poly-SiGe deposited at low temperature, it can be monolithically integrated with CMOS in the future.

© 2012 Elsevier B.V. All rights reserved.

## 1. Introduction

Integrated variable optical attenuators (VOAs) have been widely used for actively controlling the optical power level in wavelength-division multiplexing (WDM) networks [1]. The widespread deployment of WDM networks demands VOAs with compact, robust designs with low power consumption and low wavelength dependent loss (WDL) [2]. Moreover, these VOAs should be able to dynamically regulate the WDM channel power irrespective of the incident light polarization. Additionally, in dense wavelength division multiplexing (DWDM) systems, it has become common to control the output of Distributed Feedback Laser Diodes (DFB-LD) with a VOA instead of the input current. Hence, with increasing number of wavelengths multiplexed in these networks, large arrays of VOAs preferably integrated on a single silicon chip will be needed for future DWDM applications. In addition, although the VOAs are now mostly used in telecommunication applications, there are other fields where VOAs are extremely useful. E.g. the membranes used in the absorbance based optodes which are susceptible to degradation due to excessive optical power [3]. Also, with increasing popularity of Visible Light communications (VLC), use of VOAs in the visible wavelength is becoming more and more popular [4].

Basically two different families of VOAs have been presented so far, namely those based on micro-optoelectromechanical systems (MOEMS) and those based on photonic lightwave circuits (PLC). Typically, MOEMS based VOAs offer physical features such as tun-

ability, scalability, low electrical power consumption and small form factor [5]. Additionally, as the MEMS technologies use a semiconductor-like lithographic batch fabrication process, the micro-opto-mechanical components can be monolithically integrated (if the technologies used are thermally and material-wise compatible) with the control electronics on the same chip [6]. This not only improves the performance, yield and reliability but also lowers the manufacturing, packaging and instrumentation costs [7].

Out of the several different MOEMS based VOA designs proposed over the years, interference type VOAs are one of the most primitive and popular ones. The interference type VOA uses multi-beam interference to adjust the attenuation level. The first such design was the MARS (mechanical antireflection switch) modulator [8], in which a  $\text{SiN}_x$  membrane of  $\lambda/4$  optical thickness was suspended over a silicon substrate with a fixed  $3\lambda/4$  spacing. When reflections from the top surfaces of the membrane and substrate are in phase, the incident light is totally reflected. But when the membrane is electrostatically lowered to an airgap of  $\lambda/2$ , it becomes an antireflection coating with strongly reduced reflectivity. Though the achieved attenuation level was 31 dB with  $<3 \mu\text{s}$  of response time, the reported insertion loss was  $\sim 3$  dB and the device had a relatively high actuation voltage of 35.2 V. An alternative design consists of a 1D deformable grating based VOA having two sets of grating lines where one is movable and the other is fixed on the substrate [9]. A contrast of 16 dB with a much lower driving voltage of 9.6 V was reported. But, as these gratings are actually a 1D array of very closely spaced suspended microbeams with subwavelength airgap and metallic coating, the specular reflection is a strong function of the state of polarization of the incident light [10].

\* Corresponding author.

E-mail address: [sukumar.rudra@intec.ugent.be](mailto:sukumar.rudra@intec.ugent.be) (S. Rudra).

In this paper we report an alternative design which can be used effectively in solving the polarization dependence of the grating based VOAs. We used poly-SiGe as the structural material as it has been demonstrated to be an ideal material for a MEMS-last monolithic process. Since, poly-SiGe films (deposition temperature  $\sim 450^\circ\text{C}$ ) with very good electrical and mechanical properties can be obtained at CMOS-compatible temperatures [11], it is highly suited for applications that need arrays of MEMS devices to be individually connected to the interfacing circuits [12]. Our device consists of a poly-SiGe based 2D MEMS grating built from an anchored membrane with symmetrically distributed square shaped perforations which are filled with fixed islands. Because of the planar symmetry of the design, any preferential reflectivity of the different polarization states is effectively eliminated. Also, because of the relatively large dimension of these membranes, the actuation voltage is sufficiently low, leading to minimal power consumption. The design was altered in such a manner that the moving membrane exhibits the optimal damping condition leading to a minimal switching time. Using a 400 nm laser, we obtained an attenuation of  $\sim 20$  dB with a maximum polarization dependent loss of 0.11 dB and a switching time of  $\sim 3.3$   $\mu\text{s}$ . To our knowledge, this is the first functional CMOS compatible 2D MEMS grating to be reported.

## 2. Device concept

The proposed structure is presented in Fig. 1a. It consists of a suspended (anchored on four different sides) square shaped membrane which is perforated symmetrically in both the in-plane orthogonal directions. Within these perforations, fixed blocks are

created (Fig. 1b) which are supported by anchors of the same height as those supporting the membrane as shown in the cross sectional view in Fig. 1c. The design was made in such a manner that the area of the movable part and fixed parts are nearly the same. The membrane is held in tension so that it remains flat and forms a reflective surface in the non-actuated state (OFF state) giving specular reflection in the 0th order. When actuated, the membrane is deflected vertically resulting into an entirely reconfigurable 2D diffractive element (ON state) producing increased diffraction in the higher orders (Fig. 1d). At a deflection of  $\lambda/4$ , the light reflected from the membrane and the top of the islands are exactly opposite in phase which results in total annihilation of the 0th order intensity.

The electrostatic force on the membrane associated with the constant voltage drive mode is nonlinear and gives rise to the well known phenomenon of pull-in [13,14]. The electrostatically actuated membrane collapses on the ground plane once the highest deflection exceeds approximately one-third of the airgap ( $d_0$ ). Hence in the VOA structure, the airgap between the membrane and the underlying ground substrate is designed in such a manner that  $d_0/3 > \lambda/4$ . The actuation voltage is therefore always maintained well below the pull-in voltage, saving it from deterioration. The detailed background theory regarding the function of these movable gratings can be found elsewhere [15].

## 3. Device fabrication

The structural layer is a B-doped poly-SiGe layer with a thickness of 330 nm which was deposited by chemical vapor deposition

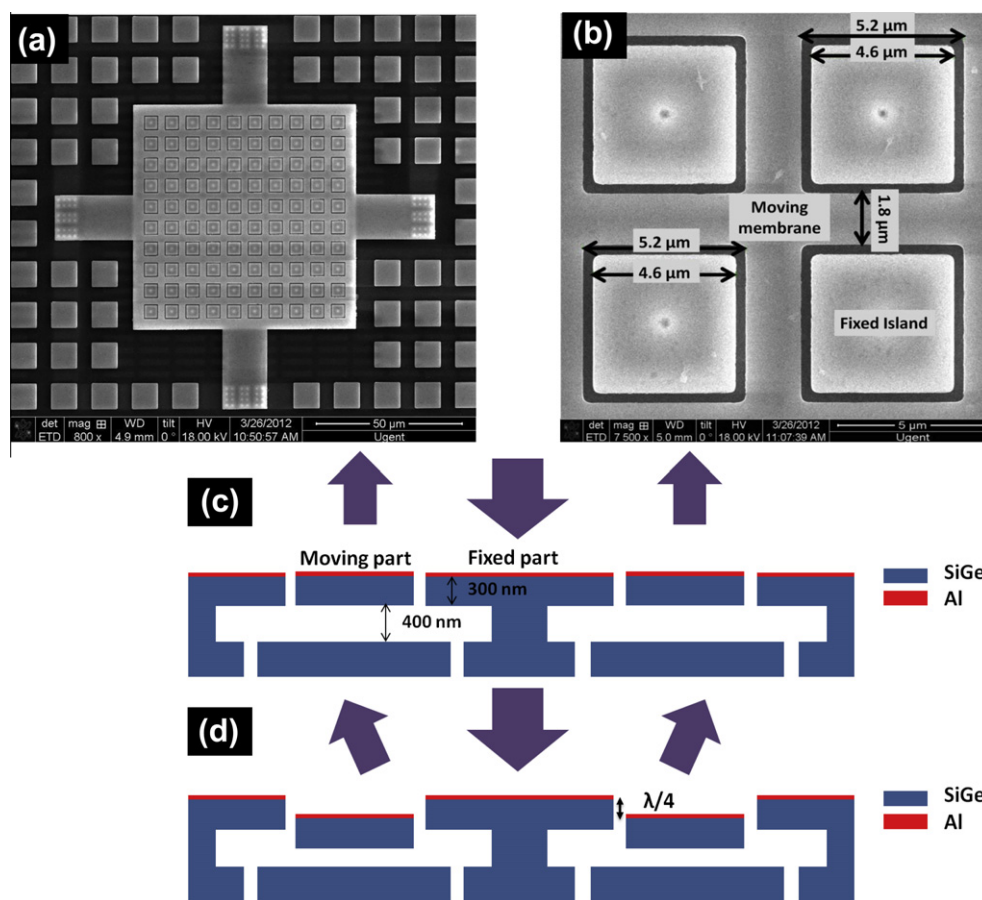


Fig. 1. SEM pictures of the top view of the full device with the attaching supports (a), zoomed-in view of the perforated membrane filled with the fixed islands (b), cross sectional schematic and working principle of the device in the non actuated state (c) and in the actuated state (d).

(CVD) at a wafer temperature of 450 °C on top of a Ti (5 nm)/TiN (10 nm) adhesion layer. The precursor gasses were SiH<sub>4</sub>, GeH<sub>4</sub> and B<sub>2</sub>H<sub>6</sub>. The SiH<sub>4</sub>:GeH<sub>4</sub> ratio equaled 0.9:1 and a B<sub>2</sub>H<sub>6</sub> (1% in H<sub>2</sub>) flow of 90 sccm was used at a wafer temperature of 450 °C, resulting in an expected Ge concentration of 78%. Next, a CMP step was used on the SiGe structural layer for roughness reduction. This CMP step also reduces the thickness of the structural layer down to 300 nm. Then a barrier layer of 5 nm thick SiC and a 30 nm thick Al layer were further added on top of the structural poly-SiGe layer to increase the reflectivity of the structures. A 400 nm airgap was maintained between the membrane and the underlying electrode. Due to limits in the lithographic resolution, the separation between the moving and the stationary part of the structural layer was fixed at 300 nm. Thickness values of the different layers and the separation among them was later confirmed by SEM cross-sectional measurements of the functional devices. A detailed description regarding the step by step fabrication of the devices can be found in our earlier report [15].

By fitting the resonance frequency of fabricated fixed–fixed beams of different lengths to simulation results, a Young's modulus of 120 GPa and a tensile stress of 20 MPa were derived for the SiGe structural layer [15]. The inherent tensile stress within the poly-SiGe layer was helpful in avoiding the initial bending of the suspended membrane and to keep it flat.

Though we used devices of different dimensions, here we discuss the best results as obtained with a perforated membrane with a total dimension of 75 × 75 μm, forming a grating with period of 7.0 μm with a fill factor of 0.88. The device is suspended on its four sides by supports of 18 × 15 μm each, which are then attached to anchors at the outer parts (Fig. 1b).

## 4. Experimental results and discussions

### 4.1. Optical characterizations

The optical characterization of the proposed design was carried out using a linearly polarized laser of 400 nm wavelength. This wavelength was selected in accordance to the airgap (400 nm) between the substrate and the membrane in the designed device. Fig. 2 shows the experimental set-up used to characterize the VOA. The two convex lenses in the front act as a collimator. The lens in front of the grating focuses the light as a circular spot (~40 μm diameter) with uniform intensity on the center of the VOA membrane. The beamsplitter helps in separating the incoming and outgoing light. A photodiode in series with a filtering slit was used to measure the intensity of the 0th diffracted order as a function of amplitude of the applied actuation voltage. Additionally, we used a quarter wave plate in front of the beamsplitter to generate

the circularly or elliptically polarized light which was used in determining the polarization dependence of the VOA performance.

The device under investigation was mounted on a XYZ stage and was monitored with a microscope which helped us in finding the optimum position (center of the membrane) of the focused spot on the membrane giving rise to the maximum achievable attenuation. As we work with the 0th diffraction order, a small change in the incidence angle does not significantly influence the efficiency and the attenuation of the gratings under investigation.

The insertion loss of the devices was found to be ~1.1 dB which is mostly associated with the fill-factor of the grating and the reflectivity of the top layer. We believe that, with finer lithographic precision, the fill factor can be increased further. Moreover, due to the higher reflectivity of Al in the NIR regime, the insertion loss will be even lower in that part of the spectrum. The attenuation as function of the applied voltage is shown in Fig. 3. A clear decrease in the 0th order intensity (increasing attenuation) can be observed with increasing external DC bias. We could obtain a maximum attenuation level of ~20 dB with an operating voltage of 1.6 V. The experimental result was also compared to a theoretical calculation carried out using Rigorous Coupled Wave Analysis (RCWA) [16]. While the qualitative behavior matches well, the maximum attenuation level differs by approximately 10 dB between the experimental results and the RCWA based simulations. To understand this discrepancy, we also performed a COMSOL Multiphysics™ based simulation studying the deflection of the membrane when applying a voltage. Fig. 4 shows that the deflection is not uniform as assumed in the RCWA simulations, but that there is a maximum deflection right at the center of the membrane. Hence, light reflected from the off-center parts is less attenuated as compared to that reflected from the center of the membrane. More importantly, due to working with the 0th order mode, the removal of stray light is more challenging in the experimental set-up and hence we experience a decreased contrast. The PDL was measured at different attenuation levels, as shown in Fig. 5. A maximum loss of 0.11 dB at the highest attenuation of 20 dB was obtained which supports our claim that this device operates as a polarization independent VOA.

One of the substantial advantages of MEMS based VOAs compared to bulk mechanical systems is their high response speed enabling faster data transfer. Hence, it was important to study the device dynamics of these MEMS gratings. Due to the small underlying airgap and fast operating speed, squeeze film damping [17] becomes the dominant damping mechanism affecting the dynamic response of the device. So, we used Laser Doppler Vibrometry (LDV) to characterize the mechanical behavior of the suspended membrane. A resonance frequency of 320 kHz was obtained for the device. We also studied the damping nature of the device through applying a square wave pulse train with 20 μs period. As

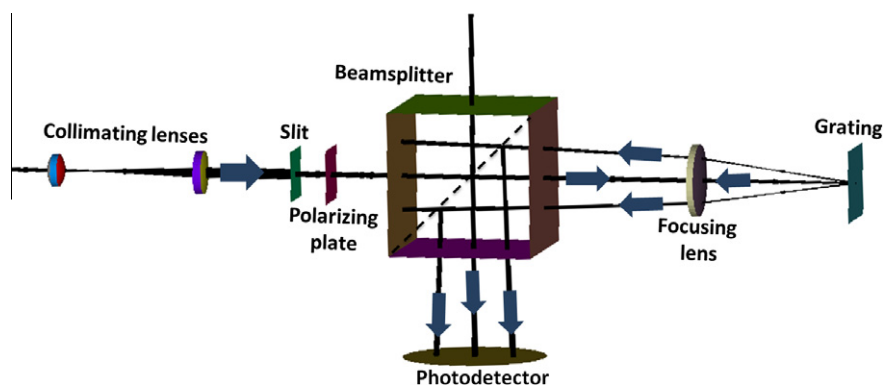


Fig. 2. Schematic of the optical set-up used to characterize the attenuation of the device.

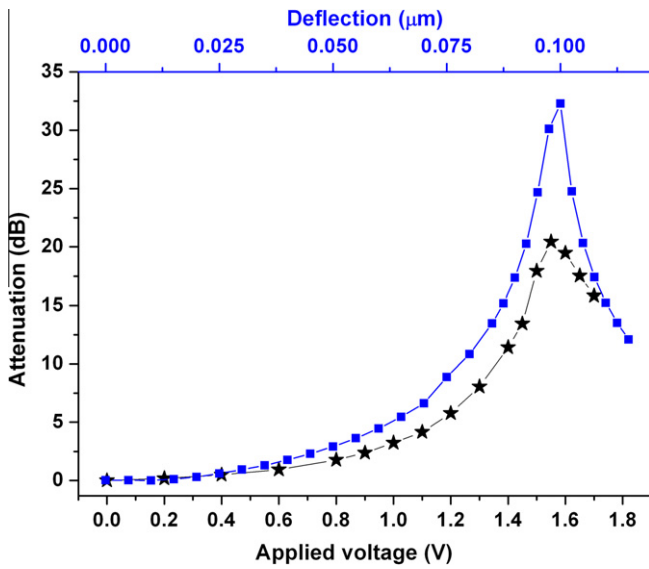


Fig. 3. Comparison of the experimental and theoretical attenuation of the proposed device.

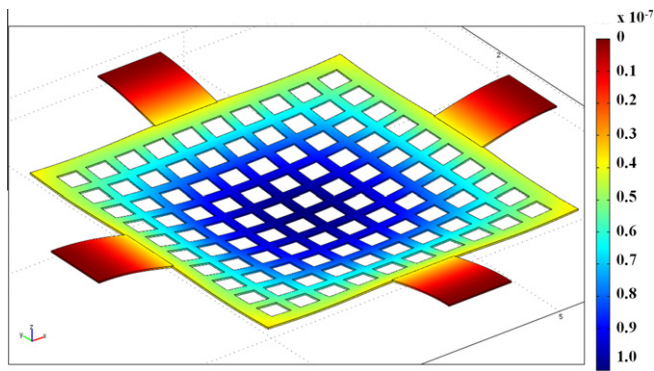


Fig. 4. COMSOL modeling of the electrostatic displacement of the membrane.

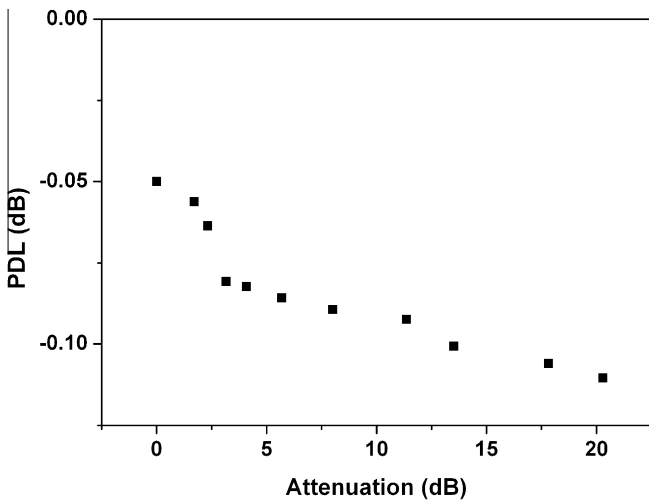


Fig. 5. Change in PDL with attenuation of the device.

evident from Fig. 6, a critically damped response was obtained for the device with a settling time  $\sim 3.3 \mu\text{s}$  (equilibrium  $\pm 2\%$ ). To cross-check the experimental result, the mechanical behavior of

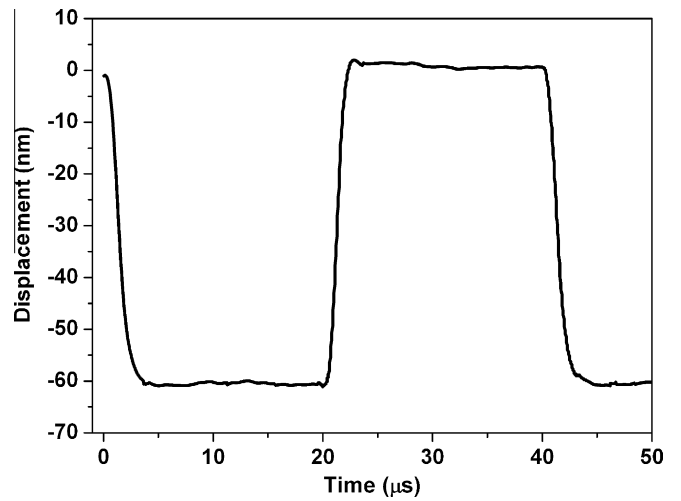


Fig. 6. Step-response to a square wave pulse train showing a critical damped nature of the device.

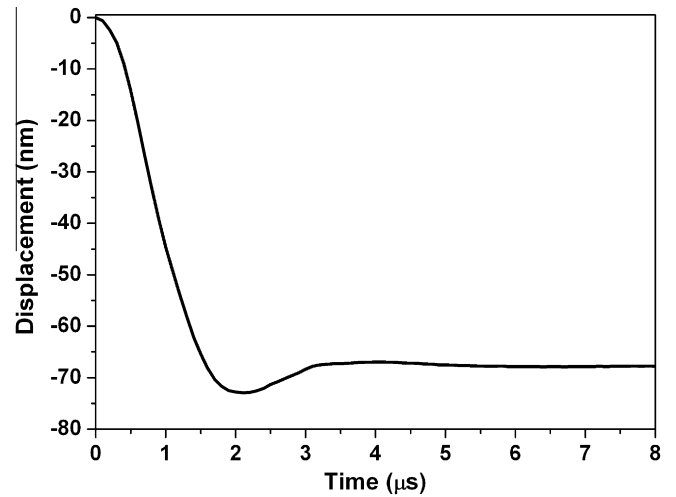


Fig. 7. Simulated step response of the device showing a near critical damped behavior.

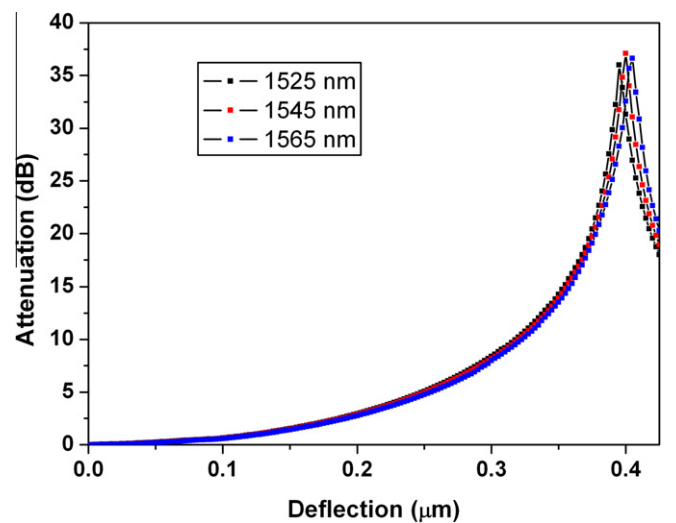


Fig. 8. Wavelength dependent attenuation characteristics of the device as simulated using RCWA.

the membrane was studied further using COMSOL. These simulations match our experimental results well with a calculated resonance frequency of 343 kHz and a near critical damped response as shown in Fig. 7. The close match between the experimental and simulated results shows that by properly optimizing the design parameters, fast settling time can be achieved even when the desired usable range is extended to the NIR regime.

We also calculated the expected wavelength dependent loss (WDL) for our devices in the C-band used for fiber based telecommunication using RCWA simulations. Fig. 8 shows the attenuation as function of the displacement of the membrane for different wavelength of the incident light. Over a 40 nm bandwidth and for an attenuation level of 15 dB there is a maximal variation of 0.9 dB.

## 5. Conclusion

We showed the operation of a 2D grating based MEMS VOA fabricated using the robust poly-SiGe technology suitable for monolithically integrating the devices directly on top of CMOS. We obtained a maximum attenuation of 20 dB for the devices with a polarization dependent loss of 0.11 dB and a settling time of  $\sim 3.3 \mu\text{s}$ . We also showed a very close overlap between the experimental and theoretical results regarding the mechanical behavior of the membrane indicating the possibility of optimizing the settling time in case of an altered design geared towards the NIR regime. Overall, these results prove the usefulness of the poly-SiGe technology in fabricating high quality VOAs. Given the compatibility of this SiGe platform with post-CMOS processing, this can be a step forward in efficiently integrating large arrays of VOAs on a single silicon chip.

## Acknowledgement

We would like to thank the Flemish agency for Innovation through Science and Technology to support this work through the SBO GEMINI project.

## References

- [1] H. Ishio, J. Minowa, K. Nosu, J. Lightwave Technol. 2 (1984) 448–463.
- [2] A. Liu, Photonics MEMS devices: Design, Fabrication and Control, CRC Press, 2009.
- [3] M. Puyol, I. Salinas, I. Garcés, F. Villuendas, A. Llobera, C. Domínguez, J. Alonso, Anal. Chem. 74 (2002) 3354–3361.
- [4] A.M. Khalid, G. Cossu, R. Corsini, M. Presi, E. Ciaramella, Hybrid Radio over Fiber and Visible Light (RoF-VLC) Communication System, in: 37th European Conference and Exposition on Optical Communications, 2011, paper We.7.C.1.
- [5] C. Lee, J.A. Yeh, J. Micro/Nanolith. MEMS MOEMS 7 (2008) 021003.
- [6] R. Jablonski, M. Turkowski, R. Szewczyk, Recent Advances in Mechatronics, Springer, 2007.
- [7] A. Witvrouw, Scr. Mater. 59 (2008) 945–949.
- [8] J.E. Ford, J.A. Walker, IEEE Phot. Tech. Lett. 10 (1998) 1440–1443.
- [9] O. Solgaard, F.S.A. Sandejas, D.M. Bloom, Opt. Lett. 17 (1992) 688–690.
- [10] E. Tamaki, Y. Hashimoto, O. Leung, Computer to plate printing using the Grating Light Valve device, in: Photonics West 2004, Micromachining and Microfabrication symposium, 2004, paper 5348–08.
- [11] S. Sedky, A. Witvrouw, K. Baert, Sen. Actuators A 97–98 (2002) 503–511.
- [12] L. Haspelslagh, J. De Coster, O.V. Pedreira, I. De Wolf, B. Du Bois, A. Verbist, R. Van Hoof, M. Willeghems, S. Locorotondo, G. Bryce, et al., Highly reliable CMOS-integrated 11MPixel SiGe-based micro-mirror arrays for high end industrial applications, in: Proceedings of IEEE Int. Electron Devices Meeting, 2008, pp. 1–4.
- [13] G.M. Rebeiz, R.F. Mems, Theory Design and Technology, John Wiley and Sons, 2003, pp. 21–31.
- [14] D. Peroulis et al., IEEE Trans. Microwave Theory Techn. 51 (2003) 259–270.
- [15] S. Rudra, J. De Coster, R. Van Hoof, G. Bryce, S. Severi, A. Witvrouw, D. Van Thourhout, Sens. Actuators A 179 (2012) 283–290.
- [16] M.G. Moharam, T.K. Gaylord, J. Opt. Soc. Am. 71 (1982) 811–818.
- [17] M. Bao, H. Yang, Sens. Actuators A 136 (2007) 3–27.